New insight into the catalytic mechanism of chorismate mutases from structural studies

Chorismate mutase catalyzes the rearrangement of chorismic acid to prephenic acid, which is the first committed step in the biosynthesis of aromatic amino acids. Its catalytic mechanism has been much studied, but is poorly understood. Recent structural information on enzymes from two species, and on an antibody that catalyzes the same reaction, has shed new light on this topic.

Chemistry & Biology April 1995, **2**:195–203

Chorismic acid is the key branch point intermediate in the shikimate pathway of bacteria, fungi, and higher plants [1]. It can be converted either into prephenic acid, eventually leading to tyrosine and phenylalanine, or into anthranilate, eventually producing tryptophan. The intramolecular rearrangement of chorismic acid to prephenic acid (Fig. 1) is catalyzed by chorismate mutase. This enzyme accelerates the reaction some two million-fold, yet, despite its central role in the aromatic biosynthetic pathway, the enzyme's catalytic mechanism remains poorly understood [2,3]. Recent structural studies on several naturally occuring chorismate mutases [4–6], and on an antibody that catalyzes the same reaction [7], may now have provided some insight into the catalytic mechanisms used by these proteins.

Interdisciplinary studies on chorismate mutase by chemists, biochemists and enzymologists have taken many forms. The kinetics of the reaction have been investigated using solvent, substituent, and isotope effects [3,8–13]; protein modification has been used to identify key amino-acid residues [14–16], and several competitive inhibitors and alternative substrates have been synthesized [17–24]. As well as these approaches, the enzyme has been studied by NMR and infrared spectroscopy [25–28], and theoretical calculations have been used to propose models for the transition state involved in rearrangement [3,29–32]. Genetic, immunological, and evolutionary analyses [33–35] have also provided information on the characteristics of the enzyme.

Efforts to mimic the catalytic mechanism of chorismate mutase have ranged from the design of simple cryptands (crypt-like, bridged crown ethers) [36] to the production of monoclonal antibodies generated against a putative transition-state analog [37,38]. Two groups have achieved antibody-mediated catalysis of the rearrangement of (–)-chorismic acid: antibody 1F7 [7,39,40] gave a rate enhancement of 250-fold, while antibody 11F1-2E11 [41] gave a 10^4-fold rate enhancement.

Structural studies on chorismate mutases

Recently, detailed structural information has been obtained on several naturally occurring chorismate mutases, and on antibody 1F7. X-ray crystal structures of the enzyme from *Bacillus subtilis* [4–6] and of antibody

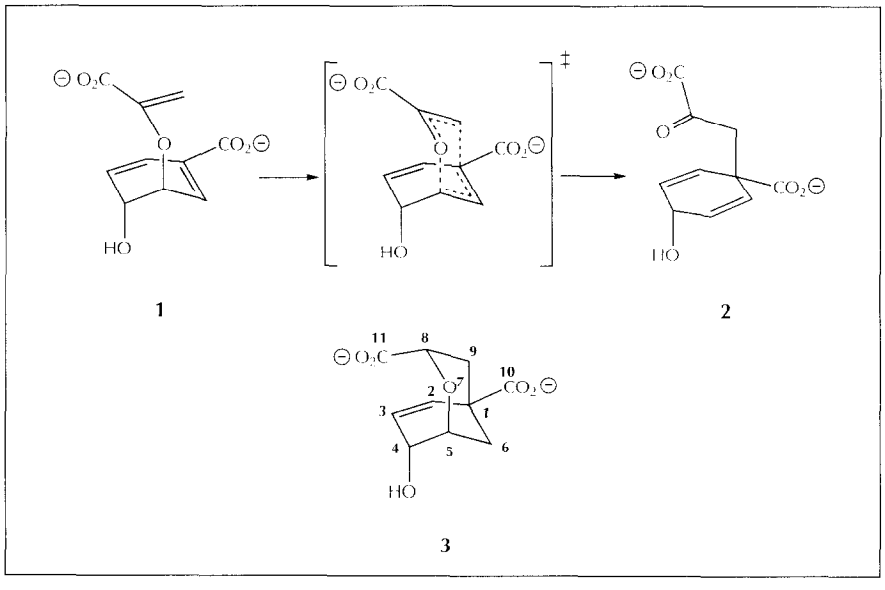

Fig. 1. The rearrangement of chorismic acid (**1**) to prephenic acid (**2**). The presumed transition state is shown, together with the transition state analog inhibitor (**3**) used in X-ray crystallographic studies. This [3,3]-pericyclic process is formally analogous to a Claisen rearrangement.

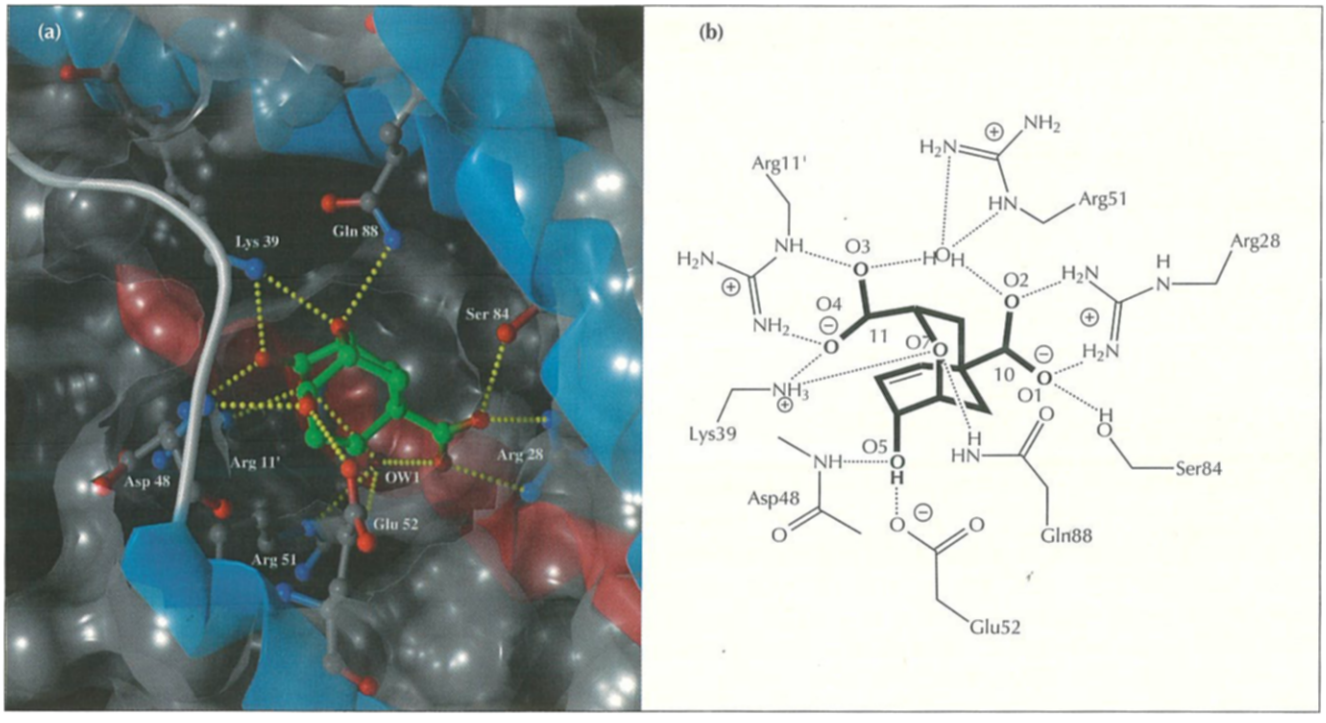

Fig. 2. The active site of *E. coli* chorismate mutase. **(a)** A space-filling model of the active site of the chorismate mutase domain of the *E. coli* P-protein complexed with transition-state analog inhibitor **3** as defined by a 2.2 Å resolution X-ray diffraction analysis [42]. **(b)** Schematic diagram of the hydrogen bonding and electrostatic interactions of the transition-state inhibitor **3** with the relevant side chains of EcCM.

1F7 [7] were obtained in complex with the inhibitor shown as compound **3** in Fig. 1. Most recently, we have been able to determine the 2.2 Å resolution X-ray structure of the monofunctional amino-terminal chorismate mutase domain (EcCM) engineered from the bifunctional *Escherichia coli* enzyme chorismate mutase-prephenate dehydratase (P-protein) [42] in complex with inhibitor **3**. Comparison of the three structures allows an informed evaluation of the various mechanistic hypotheses which have been advanced for chorismate mutase catalysis. Both the *B. subtilis* and the *E. coli* mutases appear to exploit electrostatic and hydrogen bonding effects in an unusual fashion to achieve catalysis.

The *E. coli* chorismate mutase

EcCM consists of residues 1–109 of the P-protein. It has three helical segments (residues 6–42, 49–65, 70–100) which cause the peptide backbone to adopt a shape like the figure 4. Coiled-coil and helix–helix interactions between the two longest segments create a catalytically functional, elongated homodimer with two equivalent, elbow-shaped active sites that are highly charged and completely enclosed. Although access to the active site is possible from different directions, as might be expected in the parent bifunctional enzyme, charged Arg, Asp and Glu side-chain residues on different faces of the protein shield the catalytic region from solvent (Fig. 2).

The *B. subtilis* enzyme

The *B. subtilis* chorismate mutase (BsCM) is also monofunctional, and of comparable size to EcCM. Although the kinetic parameters of EcCM and BsCM are similar, both the amino-acid sequence and the secondary structure of BsCM are strikingly different. Standard alignment methods indicate less than 20 % similarity in the EcCM and BsCM sequences (indeed, there is very little sequence similarity between any of the known mutases from different organisms). The high-resolution crystal structure of BsCM in complex with compound **3** [4,5] shows that the peptide backbone of BsCM adopts a five-stranded mixed β-sheet containing one α-helix (residues 18–34) and a two-turn 3_{10} helix. BsCM is a symmetric trimer packed to form a pseudo-α/β-barrel, with adjacent subunits forming three equivalent clefts that constitute the active sites. In striking contrast to EcCM, the active site in BsCM is open and accessible to solvent, and the protein itself makes no important contacts with the C10 carboxyl group of the inhibitor (Fig. 3).

The catalytic antibody 1F7

The three-dimensional structure of the monoclonal catalytic antibody 1F7 has been determined to 3.0 Å resolution as the Fab'-inhibitor complex [40]. Ligand binding occurs at the confluence of six loops made up of heavy (H1–H3) and light (L1–L3) chain variable domains. The active site displays a bowl-like shape or cleft, and interacts with compound **3** using a combination of electrostatic, hydrogen bonding, and hydrophobic effects (Fig. 4). As with most antibodies to small molecules, ligand complementarity resides mainly on the heavy chain; only a single residue of the light chain (Tyr-L94) interacts with compound **3**. The active site of

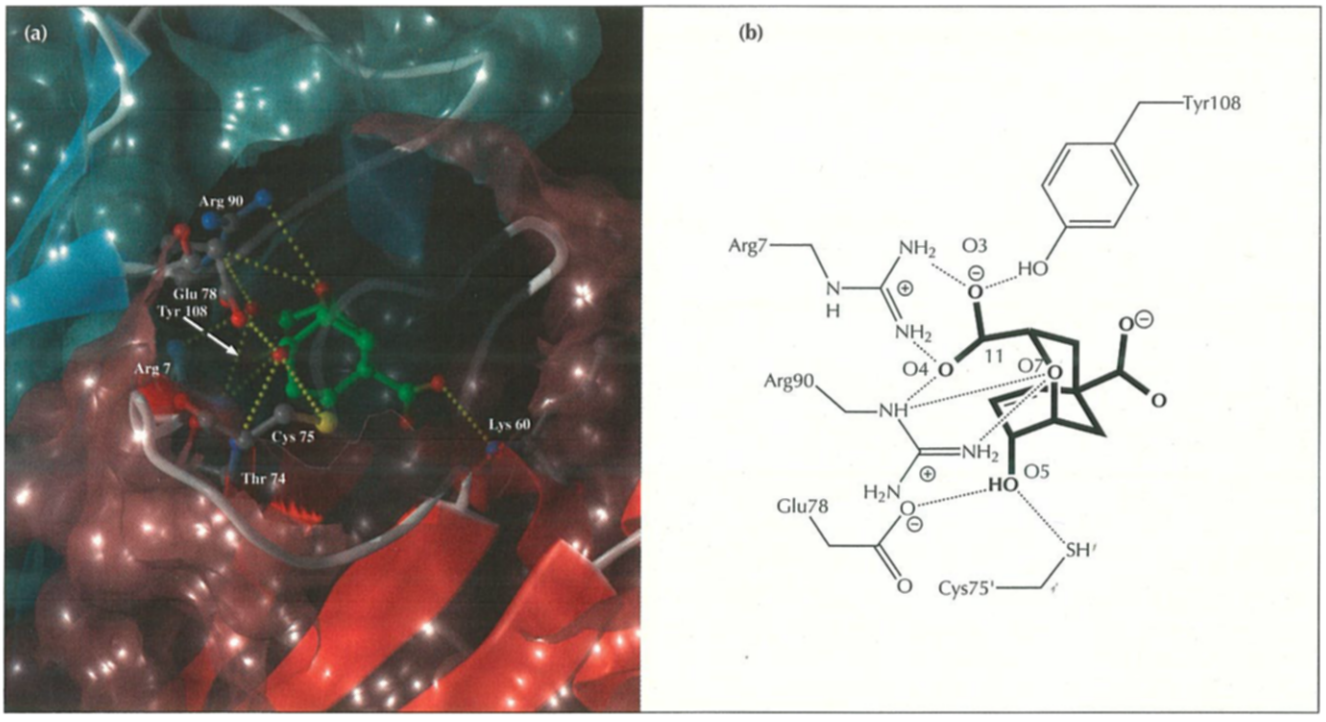

Fig. 3. The active site of *B. subtilis* chorismate mutase. **(a)** Space-filling model of the active site of *B. subtilis* chorismate mutase complexed with transition-state analog inhibitor **3** as defined by a 1.9 Å resolution X-ray diffraction analysis [4]. **(b)** Schematic diagram of the hydrogen bonding and electrostatic interactions of transition-state analog inhibitor **3** with the relevant side chains of BsCM.

1F7 thus resembles those of EcCM and BsCM in that the active sites of these enzymes are also dimeric, and the contacts again consist mainly of contributions from one monomer chain.

The rearrangement of chorismate to prephenate is a one substrate–one product process, and is one of very few chemical transformations where the enzymatic process can be compared directly with its unimolecular solution counterpart. The uncatalyzed rearrangement of chorismate to prephenate occurs about 10^3 times faster than the rearrangement of allyl vinyl ether [20,43], and for this reason has attracted considerable interest. It seems reasonable that an understanding of the intrinsically fast rearrangement of chorismate might shed light on, or provide clues about, the nature and role of substrate and transition-state binding interactions in the mutase process.

Both the enzymatic and non-enzymatic reactions proceed via chair-conformation transition structures [10,11]. Secondary tritium isotope effects on the uncatalyzed rearrangement are evident at C5 (C–O bond-breakage), but not at C9 (C–C bond formation) [9]. No comparable isotope effect is seen in the mutase-catalyzed rearrangement, although a small (k_H/k_T = 0.96) inverse secondary isotope effect is observed by tritiation at C4 [12]. Judging from activation parameters for a variety of catalysts (Table 1), and assuming that activation parameters for EcCM and BsCM resemble the other native enzymes shown in Table 1, the ability of mutases to restrict conformational degrees of freedom is important in promoting rearrangement. In the case of 1F7, however, the activation parameters suggest that the antibody's modest rate acceleration results from a reduction in $\Delta H^{\ddagger}$ for the reaction [39] rather than from entropic control.

Substrate conformation

How does chorismate mutase achieve the experimentally observed enhancement in the rate of chorismate rearrangement? Several possible ways have been suggested. Since the entropy of activation is reduced effectively to zero in the catalyzed process (Table 1), the enzyme–substrate complex must orient the ring of the substrate in the pseudo-diaxial conformation, while rotation about C5–O7 and C8–O7 must be severely restricted to lock the enol pyruvate side chain in the rearranging chair conformer. As 10–20 % of chorismate exists as the pseudo-diaxial form in dynamic equilibrium

Table 1. Activation enthalpy and entropy for the rearrangement of compound **1** to compound **2**.

Catalyst	$\Delta H^{\ddagger}$ (kcal mol^{-1})	$\Delta S^{\ddagger}$ (e.u.)	References
S. aureofaciens	14.5	–2.2	2
A. aerogenes	15.9	–1.1	2
1F7	15	–22	37
11F1-2E11	18.3	–1.2	38
Uncatalyzed	20.5	–12.9	7,16

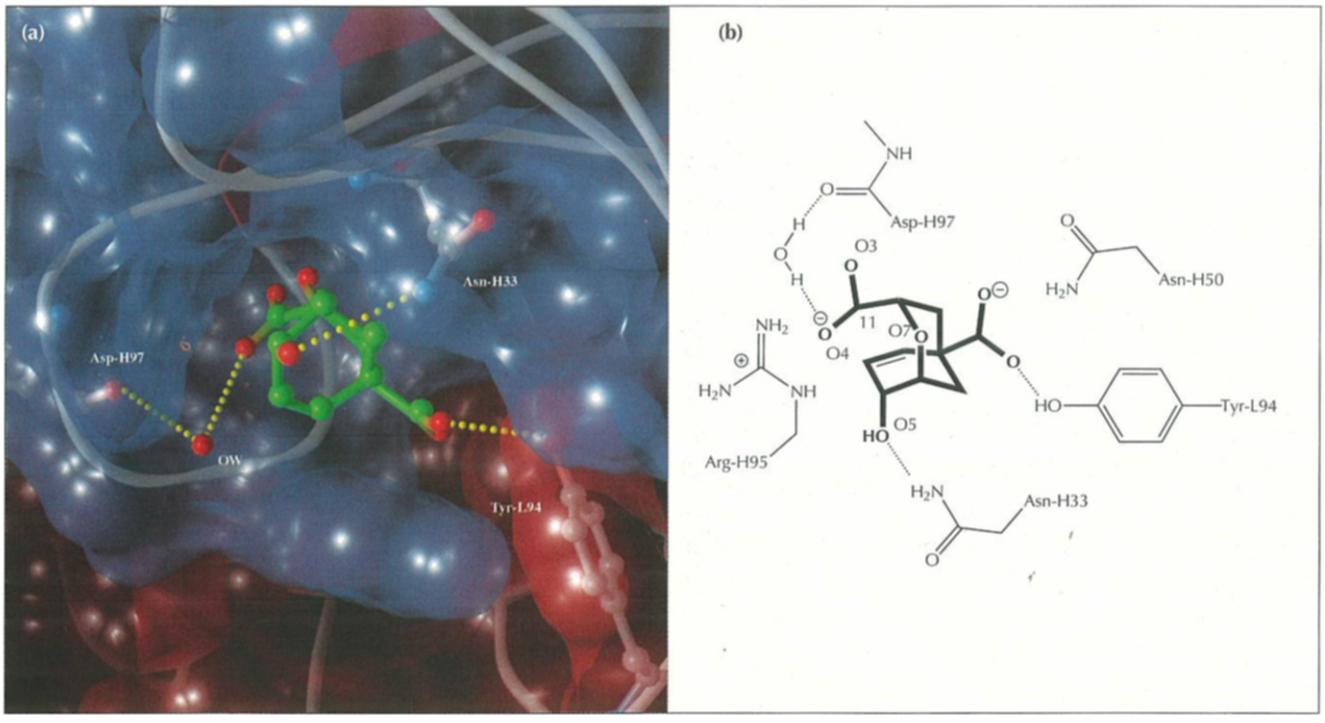

Fig. 4. The active site of antibody 1F7. **(a)** Space-filling model of the binding site of antibody 1F7, which has chorismate mutase acitivity, complexed with transition-state analog inhibitor **3** as defined by a 3.0 Å resolution X-ray diffraction analysis [40]. **(b)** Schematic diagram of the hydrogen bonding and electrostatic interactions of transition-state analog inhibitor **3** with the relevant side chains of antibody 1F7. L, light chain residue; H, heavy chain residue. Antibody 1F7 was generated by linking hapten 3 at the C4-hydroxyl group to a carrier protein, thus biasing the mode of ligand binding.

with the pseudo-diequatorial form, Knowles and colleagues [25] have suggested that the enzyme binds the diaxial conformer, and that the enzyme–substrate complex then undergoes rearrangement via some intermediate from which product formation is rapid. The inverse secondary tritium kinetic isotope effect at C4 noted earlier is thus rationalized in terms of the effect of tritium on the conformational equilibrium of chorismate (T prefers to be equatorial; thus, $k_H/k_T = 0.95$).

Enzyme–substrate binding

The functional groups of chorismate offer several possibilities for noncovalent binding in the enzyme–substrate complex (see Fig. 1). For example, the two charged carboxylate groups are capable of strong electrostatic interactions with protonated active-site residues. Suitable partners may also form H-bonds with chorismate's carboxyl and hydroxyl groups. Inhibition studies with both aliphatic and aromatic diacids indicate that the vinyl ether oxygen is important [21,24], and that hydrophobic forces may contribute to binding [2]. Finally, there is the possibility of π-electron interactions with chorismate's diene system [2].

There have been a number of attempts to observe the enzyme–substrate complex and other ligand interactions directly using ^{13}C-NMR [26,27]. Although neither free nor bound chorismate can be detected, difference spectra reveal significant perturbations between C5 and C6 in bound prephenate, perhaps caused by changes in electron density and/or molecular geometry in that region [27,28]. In support of the role of electrostatic interactions, studies using synthetic analogs and esters of chorismate indicate that the only functional groups required on the allyl vinyl ether framework in chorismate for mutase-catalyzed rearrangement are the two carboxylic acid groups [23].

The X-ray crystal structures of EcCM and BsCM provide useful information on enzyme–substrate complex formation. When the two active sites are compared by superimposing the atoms of the bound inhibitor, compound **3**, a common motif emerges in the highly charged region created by the presence of adjacent, protonated residues (Lys39, Arg11' and Arg51 in EcCM; Arg90 and Arg7 in BsCM). This electropositive wall interacts strongly with the left flank (C1–C4) of chorismate through an elaborate network of bridging H-bonds involving both O7 and the C11 carboxylate of the enol pyruvate (Figs 2b, 3b). In retrospect, an early clue to this concentration of positive charge came from the work of Gorisch, who concluded from inhibition of the *Streptomyces aureofaciens* mutase by small inorganic anions that at least two cationic groups were present in the active site [2]. Working with *E. coli* chorismate mutase-prephenate dehydratase (the source of EcCM), Gething and Davidson [15] further noted the singular importance of a lysine residue (almost certainly Lys39; Fig. 2b) whose modification led to complete loss of mutase activity without affecting the dehydratase domain.

Conformational trapping

Besides promoting enzyme–substrate complex formation through electrostatic effects, the positively charged residues in the EcCM active site are strategically arranged to orient and lock chorismate in the requisite chair conformer for rearrangement. We propose that free chorismate may enter the active site in extended conformation, shown as structure **4** in Figure 5, which minimizes electrostatic and π–π repulsive interactions. Initial contact between the enol pyruvate carboxylate and Lys39 forms an electrostatic bond. Clockwise rotation about C5–O7 enables the side-chain carboxylate group to form a second H-bond to Arg11', as shown in structure **5**. Further clockwise rotation forms the highly stabilized guanidine-carboxylate pairing shown in structure **6**, together with a third H-bond between O4 and Lys39, effectively freezing the rotation of the carboxylate group about C8–C11 and suspending the enol ether π-system over the carbocyclic ring, approximately parallel to an axis defined by C2–C4. An incremental rotation about C5–O7 forms a fourth H-bond between O3 and the tightly bound water molecule bridging Arg11' and Arg51. With its structure gradually made more compact through favorable H-bonding and electrostatic effects, chorismate is thus drawn deeper into the active site as the rearranging conformation is achieved in the enzyme–substrate complex. At the same time, an electron lone pair on O7 becomes accessible for H-bonding to Lys39 and Gln88 of EcCM (see structure **7**; this will be discussed further below).

Comparable entropic restriction of chorismate by BsCM could also result from similar interactions between the C11 carboxylate of chorismate (see Fig. 1) and Arg90, Arg7 and Tyr108, which bring O7 into proximity with Asp48 and Glu52. Antibody 1F7, however, contains only a single cationic residue (Arg-H95). The X-ray structure of 1F7 with bound compound **3** indicates just two H-bonds to the C11 carboxylate, and no side-chain residues are within H-bonding distance of O7. Instead of acting like an entropy trap, this protein displays an unfavorable decrease in $\Delta S^{\ddagger}$ (Table 1).

What is the role of the C10 carboxylate ion in substrate binding? It has been shown that the *E. coli* enzyme will not catalyze the rearrangement of dimethyl chorismate, C10-monomethyl or C11-monomethyl chorismate [23]. This absolute requirement of EcCM for both of the carboxylic acid groups of chorismate is perhaps not surprising in view of the additional H-bonding interactions between Arg28 and Ser84 and the C10 carboxylate of compound **3** (Fig. 2b). In contrast, BsCM forms no active site contacts with the ring carboxyl group of the substrate, and it is not known whether this enzyme can promote the rearrangement of C11-monomethyl chorismate. Given the quite similar steady-state kinetic profiles of BsCM (k_{cat} = 50 s^{-1}; K_M = 100 μM) [44] and EcCM (k_{cat} = 72 s^{-1}, K_M = 290 μM) [45] and their comparable behavior with inhibitor **3** (K_I = 3 μM for BsCM; K_I = 2 μM for EcCM) (H.B. Wood, Jr & B.G., unpublished

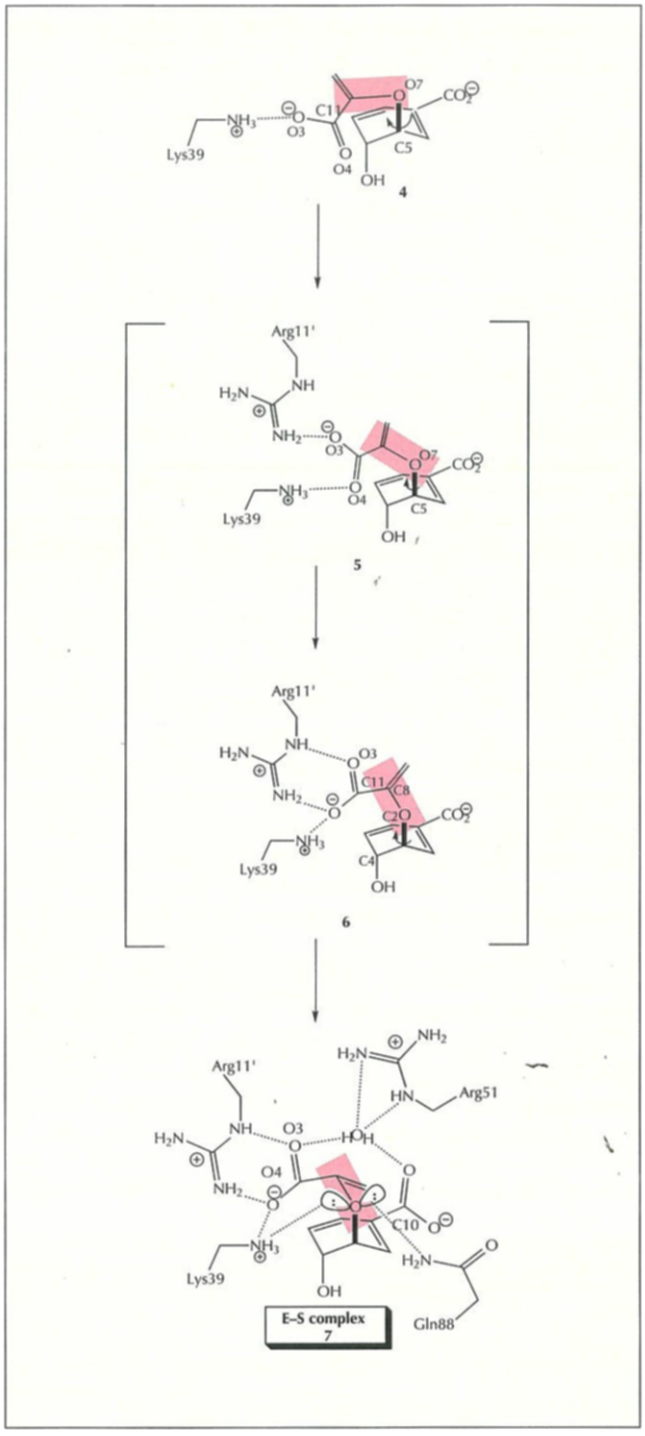

Fig. 5. Conformational trapping of chorismate during the formation of the complex with EcCM. Chorismate may initially bind in an extended conformation (structure **4**), forming an initial hydrogen bond between O3 and Lys39. Rotation around the C5–O7 bond then allows formation of a second hydrogen bond; O4 replaces O3 in the hydrogen bond to Lys39, while O3 moves to hydrogen-bond to Arg11′ (structure **5**). Further rotation around the C5–O7 bond moves O3 to yet another position (structure **6**) and increases the number of hydrogen bonds formed to three. Rotation is highlighted by the shaded rectangle, whose long axis lies along the O7–C8 bond. Once the rotation is complete, a lone pair of electrons becomes accessible for hydrogen bonding to Lys39 and Gln88 (structure **7**). At this point, the substrate is essentially frozen in a conformation close to that of the transition state. E–S complex, enzyme–substrate complex.

data) it seems probable that the two enzymes have similar mechanisms; this would imply that the C10 carboxylate has a relatively minor role in substrate binding for both enzymes.

Complexes of EcCM or BsCM with substrate may also derive additional noncovalent stabilization from the formation of two H-bonds with the C4 allylic alcohol (O5). In EcCM, O5 has one H-bond each with Asp48 and with the γ-carboxyl of Glu52 (Fig. 2). Comparable H-bonds are seen with Glu78 and Cys75' in BsCM (Fig. 3). The importance of these interactions in enzyme–substrate complexation is not clear. In the case of the *E. coli* bifunctional enzyme chorismate mutase-prephenate dehydrogenase (the T-protein: a second mutase similar to the P-protein), the C4 hydroxyl of chorismate is apparently not essential for substrate binding, since both 4-deoxychorismate and chorismate methyl ether are substrates for mutase-catalyzed rearrangement [23]. Comparable tests with these substrates using BsCM have not been reported. However, indirect evidence from studies on the *E. coli* T-protein suggest that Cys75' in BsCM is important in binding chorismate. Of the four cysteines identified in the T-protein, alkylation of one with iodoacetamide results in complete loss of mutase activity [16]. Since only one cysteine (Cys96) is found in the amino-terminal (i.e. mutase) domain of the T-protein, that residue may have a role comparable to that of Cys75' in BsCM. Similar modification studies on the *E. coli* P-protein (from which EcCM originates) indicate that none of the four cysteines in the structure is directly involved in mutase activity [16].

The catalytic mechanism

Historically, most mechanistic hypotheses about chorismate mutase have considered both carboxylic acid groups in the substrate to be important. Gorisch [2] proposed that chorismate binds the enzyme through ionic interactions at both carboxylates, with the requisite diaxial conformation gaining further stabilization from H-bonding. Alternatively, the enzyme–substrate complex, with salt bridges to both carboxylate anions restricting rotational freedom, may undergo a macromolecular conformational change. According to this hypothesis, a torque is exerted on chorismate's allyl vinyl ether system, forcing C1 and C9 closer together to facilitate rearrangement. Despite their elegance and simplicity, both of these hypotheses are invalidated by the fact that the C10 carboxylate in BsCM, insofar as can be determined from the X-ray structural data (Fig. 3), makes no significant bonding contacts with the enzyme [4,5].

Knowles and colleagues considered a mechanism in which anchimeric assistance by chorismate's C4 hydroxyl might result in transient formation of an oxirinium ion [12]. This mechanism cannot, however, explain the catalyzed rearrangement of 4-deoxychorismate and chorismate methyl ether mentioned earlier [23]. A rate-enhancing solvolysis of the C4-hydroxyl group, based on known substituent effects in pericyclic processes [43,46], is also excluded by the viability of 4-deoxychorismate as a mutase substrate ($k_{cat} \geq 1\ s^{-1}$; k_{cat} for chorismate $= 51\ s^{-1}$) [12,23].

A nucleophile-assisted, dissociative pathway for chorismate mutase-prephenate dehydrogenase mediated rearrangement has also been considered [12]. This hypothesis relies on the fact, first noted almost forty years ago by Goering and Jacobson [47] and independently by White *et al.* [48], that some Claisen rearrangements are more rapid in polar solvents. These processes are currently thought to involve dipolar or dissociated transition states [20,49], although Gajewski and colleagues [50,51] have argued that the magnitude of the observed solvent effect is substantially weaker than would be expected if bond heterolysis were important. As depicted in structure **8** (Fig. 6), the enzyme–substrate complex could undergo rate-limiting, heterolytic cleavage of the ether bond with general acid catalysis. Concomitant attack by an enzyme nucleophile leads to the covalently bound intermediate **9** which then forms

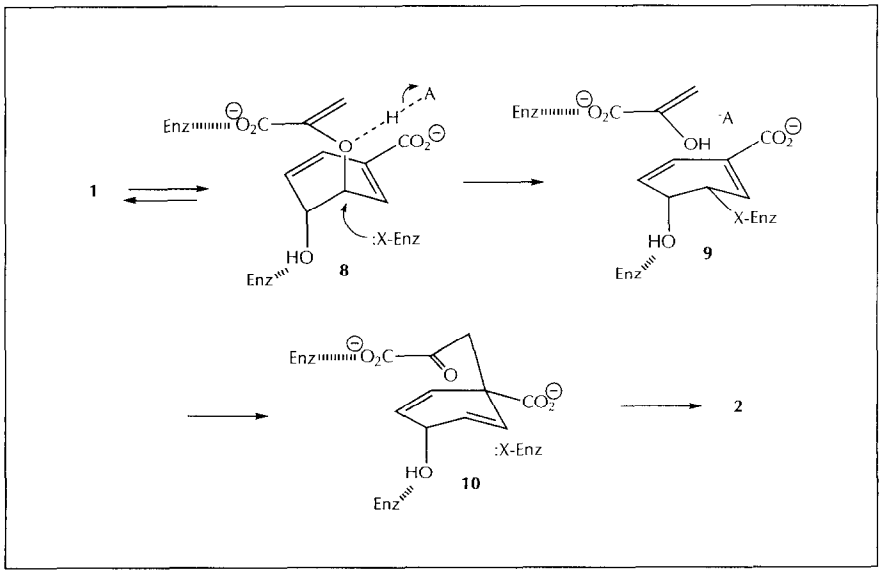

Fig. 6. Hypothetical nucleophile-assisted pathway for chorismate mutase-prephenate dehydrogenase involving a dissociative transition state (see [12]). The enzyme–substrate complex could be cleaved by a nucleophilic attack from the enzyme (see structure **8**) leading to a covalently bound intermediate (structure **9**). The product could then be formed by expelling the nucleophile in an S_N2' process.

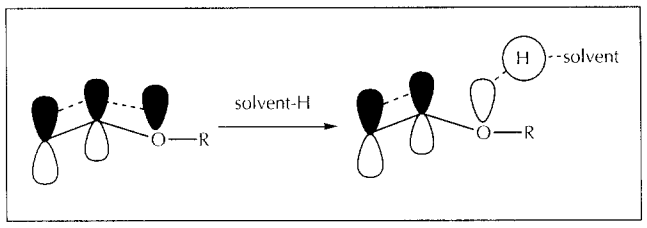

Fig. 7. An orbital diagram of n–π* conjugation in vinyl ethers, showing how hydrogen bonding disrupts the favorable resonance interaction.

product by expelling the nucleophile in an S_N2' process. The observation of a significant D_2O solvent isotope effect for the T protein (>2 on both k_{cat} and k_{cat}/K_M) is consistent with a general acid-proton transfer in the rate-limiting step.

In the case of BsCM, however, no D_2O solvent isotope effect is observed, and the enzymatic reaction is insensitive to acid or base [26]. Although mechanistic deductions based on solvent isotope effects are risky, the fact that no significant change in k_{cat}/K_M is evident between pH 5–9 with BsCM argues against the participation of an ionizable nucleophilic group, including Cys75'. Gray and Knowles [28] conclude from kinetic and spectroscopic parameters that the mutase reaction is an encounter-controlled pericyclic process, although perhaps asynchronous like its uncatalyzed counterpart. The enzymatic rearrangement is thought to be accelerated by selective binding of the reactive pseudodiaxial chair conformer, with some rate enhancement possible as a result of electrostatic stabilization of the transition state [28].

Hydrogen bonding

X-ray crystallographic studies on EcCM and BsCM inhibitor complexes reveal another common structural motif which may be responsible for the lower $\Delta H^{\ddagger}$ of the catalyzed reaction. Each enzyme forms two H-bonds with O7 of the bound inhibitor (Figs 2b, 3b). In a recent Monte Carlo simulation of the effect of hydration on Claisen rearrangements, Severance and Jorgensen [52] show that the transition state for allyl vinyl ether rearrangement in water is better hydrated than the reactant. The authors suggest that enhanced hydration, that is, increased H-bonding in water, may account for a several hundredfold rate enhancement over the Claisen rearrangement of allyl vinyl ether in the gas phase. By disrupting the well known n–π* conjugation in vinyl ethers [53], H-bonding would raise the energy of the reactant and reduce the activation enthalpy for rearrangement (Fig. 7).

Thus, two effects might explain the observed acceleration of Claisen rearrangements in polar solvents: (i) stabilization of a heterolytic transition state through solvent-promoted dissociation, and/or (ii) destabilization of the reactant through hydrogen bonding with water or alcohols. Besides accommodating the concerns of Gajewski and colleagues over the magnitude of the observed solvent effects [50, 51], this hydrogen-bonding effect suggests how chorismate mutases might reduce $\Delta H^{\ddagger}$. In the case of EcCM, formation of the enzyme–substrate complex **7** (Fig. 5) rotates the lone pairs on O7 of chorismate into position for H-bonding with Lys39 and Gln88. By disrupting n–π* conjugation in the conformationally constrained vinyl ether, H-bonding by these residues would raise the free energy of the enzyme–substrate complex and reduce the activation enthalpy for rearrangement.

The specific hydrogen bonds formed would depend on the detailed structure of the enzyme–substrate complex. If bound chorismate is conformationally constrained without H-bonding at O7, then two new H-bonds with Lys39 and Gln88 created in the transition state will significantly accelerate the rearrangement of chorismate. For $\Delta S^{\ddagger}$ to remain zero, however, a corresponding number of H-bonds must be broken elsewhere in the rearrangement transition structure. Alternatively, some H-bonding to O7 already present in the EcCM enzyme–substrate complex may become more pronounced as the rearrangement proceeds, with a compensatory weakening in H-bonding elsewhere in the transition state, most likely in the C11-carboxyl group as the enol pyruvate side chain migrates to C1.

In the case of BsCM, O7 may likewise form two hydrogen bonds with Arg90 to promote the pericyclic rearrangement, while maintaining $\Delta S^{\ddagger} \sim 0$ by forfeiting hydrogen bonds elsewhere in the active site. In antibody 1F7, however, there are no residues proximal to O7 that are capable of forming even one H-bond to the vinyl ether moiety (Fig. 4).

Thus we propose that (i) adjacent, protonated, active site residues exert conformational control in the chorismate mutase enzyme–substrate complex, and (ii) hydrogen bonding between active site residues and O7 of bound chorismate catalyzes the rearrangement step. Both mechanistic hypotheses are consistent with all available experimental data on the chorismate mutase reaction, and are amenable to experimental tests on several fronts. These hypotheses also suggest what to look for in the modest sequence similarities found to date in known mutases. One may further expect that antibody 11F1-2E11 (which enhances rearrangement by 10^4) will display one or more of the key elements that are found in the enzyme structures when the solid-state structure of this protein is elucidated.

Future possibilities

Striking differences between the shallow, exposed active site of BsCM and the enclosed, but more spacious, active site of EcCM suggest the possibility of designing species-specific mutase inhibitors. More interestingly, these findings suggest that with proper placement of charged groups in the substrate, new enzymes may be engineered to promote a wide range of pericyclic rearrangements based on similar catalytic motifs.

It is also possible that understanding how chorismate mutase catalyzes its rearrangement may allow the development of rational approaches to the next generation of mutase inhibitors. Such inhibitors could be important leads for new antibiotics and herbicides. The shikimate pathway is the effective site of action of such successful drugs as trimethoprim (an inhibitor of dihydrofolate reductase) and the sulfa antibiotics (p-aminobenzoate mimics which disrupt folate biosynthesis). Chorismate mutase inhibitors could join the ranks of these therapeutic agents, either as stand-alone drugs or as part of a dual-blockade strategy for antibiotic chemotherapy. In either case, mutase inhibitors represent a form of treatment against which no resistance mechanisms have yet emerged.

Acknowledgements: This work was supported by NIH GM24054 (BG) and CA24487 (JC). We also thank Dr Richard Gillilan of the Cornell Theory Center and Mr Ping Kongsaeree for their enthusiastic help with the graphics.

References

1. Haslam, E. (1993). *Shikimic Acid Metabolism and Metabolites* John Wiley & Sons, New York.
2. Gorisch, H. (1978). On the mechanism of the chorismate mutase reaction. *Biochemistry* **17**, 3700–3705.
3. Andrews, P.R., Smith, G.D. & Young, I.G. (1973). Transition state stabilization and enzymic catalysis. Kinetic and molecular orbital studies of the rearrangement of chorismate to prephenate. *Biochemistry* **12**, 3492–3498.
4. Chook, Y.-M., Ke, H. & Lipscomb, W.N. (1993). Crystal structures of the monofunctional chorismate mutase from *Bacillus subtilis* and its complex with a transition state analog. *Proc. Natl. Acad. Sci. USA* **90**, 8600–8603.
5. Chook, Y.-M., Gray, J.V., Ke, H. & Lipscomb, W.N. (1994). The monofunctional chorismate mutase from *Bacillus subtilis*. Structure determination of chorismate mutase and its complexes with a transition state analog and prephenate, and implications for the mechanism of the enzymatic reaction. *J. Mol. Biol.* **240**, 476–500.
6. Xue, Y., Lipscomb, W.N., Graf, R., Schnappauf, G. & Braus, G. (1994). The crystal structure of allosteric chorismate mutase at 2.2 Å resolution. *Proc. Natl. Acad. Sci. USA* **91**, 10814–10818.
7. Hilvert, D. & Nared, K.D. (1988). Stereospecific Claisen rearrangement catalyzed by an antibody. *J. Am. Chem. Soc.* **110**, 5593–5594.
8. Heyde, E. & Morrison, J.F. (1978). Kinetic studies on the reactions catalyzed by chorismate mutase-prephenate dehydrogenase from *Aerobacter aerogenes*. *Biochemistry* **17**, 1573–1580.
9. Addadi, L., Jaffe, E.K. & Knowles, J.R. (1983). Secondary tritium isotope effects as probes of the enzymic and nonenzymic conversion of chorismate to prephenate. *Biochemistry* **22**, 4494–4501.
10. Sogo, S.G., Widlanski, T.S., Hoare, J.H., Grimshaw, C.E., Berchtold, G. A. & Knowles, J.R. (1984). Stereochemistry of the rearrangement of chorismate to prephenate. Chorismate mutase involves a chair transition state. *J. Am. Chem. Soc.* **106**, 2701–2703.
11. Copley, S.D. & Knowles, J.R. (1985). The uncatalyzed Claisen rearrangement of chorismate to prephenate prefers a transition state of chairlike geometry. *J. Am. Chem. Soc.* **107**, 5306–5308.
12. Guilford, W.J., Copley, S.D. & Knowles, J.R. (1987). On the mechanism of the chorismate mutase reaction. *J. Am. Chem. Soc.* **109**, 5013–5019.
13. Delany, J.J., Padykula, R.E. & Berchtold, G.A. (1992). Uncatalyzed and chorismate mutase catalyzed Claisen rearrangements of 5,6-dihydrochorismate and 6-oxa-5,6-dihydrochorismate. *J. Am. Chem. Soc.* **114**, 1394–1397.
14. Gething, M.-J. & Davidson, B.E. (1977). Chorismate mutase-prephenate dehydratase from *Escherichia coli* K12. Modification with 5,5'-dithio-bis(2-nitrobenzoic acid). *Eur. J. Biochem.* **78**, 103–110.
15. Gething, M.-J. & Davidson, B.E. (1977). Chorismate mutase-prephenate dehydratase from *Escherichia coli* K12. Effect of chemical modification on the enzymic activities and allosteric inhibition. *Eur. J. Biochem.* **78**, 111–117.
16. Hudson, G.S., Wong, V. & Davidson, B.E. (1984). Chorismate mutase/prephenate dehydrogenase from *Escherichia coli* K11: purification, characterization, and identification of a reactive cysteine grouping. *Biochemistry* **23**, 6240–6249.
17. Andrews, P.R., Cain, E.N., Rizzardo, E. & Smith, G.D. (1977). Rearrangement of chorismate to prephenate. Use of chorismate mutase inhibitors to define transition state structure. *Biochemistry* **16**, 4848–4852.
18. Chao, H.S.-I. & Berchtold, G.A. (1982). Inhibition of chorismate mutase activity of chorismate mutase-prephenate dehydrogenase from *Aerobacter aerogenes*. *Biochemistry* **21**, 2778–2781.
19. Christopherson, R.I. & Morrison, J.F. (1985). Chorismate mutase-prephenate dehydrogenase from *Escherichia coli*: positive cooperativity with substrates and inhibitors. *Biochemistry* **24**, 1116–1121.
20. Gajewski, J.J., *et al.*, & Carpenter, B. K. (1987). On the mechanism of rearrangement of chorismic acid and related compounds. *J. Am. Chem. Soc.* **109**, 1170–1186.
21. Bartlett, P.A., Nakagawa, Y., Johnson, C.R., Reich, S.H. & Luis, A. (1988). Chorismate mutase inhibitors: synthesis and evaluation of some potential transition state analogues. *J. Org. Chem.* **53**, 3195–3210.
22. Pawlak, J.L. & Berchtold, G.A. (1988). Synthesis of disodium 3-[(1-carboxylatoethenyl)-oxy]cyclohepta-1,6-diene-1-carboxylate: a seven-membered ring analogue of chorismate. *J. Org. Chem.* **53**, 4063–4069.
23. Pawlak, J.L., *et al.*, & Berchtold, G.A. (1989). Structural requirements for catalysis by chorismate mutase. *J. Am. Chem. Soc.* **111**, 3374–3381.
24. Clarke, T., Stewart, J.D. & Ganem, B. (1990). Transition state analogue inhibitors of chorismate mutase. *Tetrahedron* **46**, 731–748.
25. Copley, S.D. & Knowles, J.R. (1987). The conformational equilibrium of chorismate in solution: implications for the mechanism of the non-enzymic and the enzyme-catalyzed rearrangement of chorismate to prephenate. *J. Am. Chem. Soc.* **109**, 5008–5013.
26. Gray, J.V., Eren, D. & Knowles, J.R. (1990). Monofunctional chorismate mutase from *Bacillus subtilis*: Kinetic and ^{13}C-NMR studies on the interactions of the enzyme with its ligands. *Biochemistry* **29**, 8872–8878.
27. Rajagopalan, J.S., Taylor, K.M. & Jaffe, E.K. (1993). ^{13}C-NMR studies of the enzyme-product complex of *Bacillus subtilis* chorismate mutase. *Biochemistry* **32**, 3965–3972.
28. Gray, J.V. & Knowles, J.R. (1994). Monofunctional chorismate mutase from *Bacillus subtilis*: FTIR studies and the mechanism of action of the enzyme. *Biochemistry* **33**, 9953–9959.
29. Andrews, P.R. & Haddon, R.C. (1979). Molecular orbital studies of enzyme-catalyzed reactions. Rearrangement of chorismate to prephenate. *Aust. J. Chem.* **32**, 1921 1929.
30. Andrews, P.R. & Heyde, E. (1979). A common active site model for catalysis by chorismate mutase-prephenate dehydrogenase. *J. Theor. Biol.* **78**, 393–403.
31. Wiest, O. & Houk, K.N. (1994). On the transition state of the chorismate-prephenate rearrangement. *J. Org. Chem.* **59**, 7582–7584.
32. Yo, H.Y. & Houk, K.N. (1994). Transition structures and kinetic isotope effects for the Claisen rearrangement. *J. Am. Chem. Soc.* **116**, 12047–12048.
33. Ahmad, S., Wilson, A.-T. & Jensen, R.A. (1988). Chorismate mutase:prephenate dehydratase from *Acinetobacter calcoaceticus*: purification, properties, and immunological cross-reactivity. *Eur. J. Biochem.* **176**, 69–79.
34. Schmidheini, T., Sperisen, P., Paravinici, G., Hutter, R. & Braus, G. (1989). A single point mutation results in a constitutively activated and feedback-resistant chorismate mutase of *Saccharomyces cerevisiae*. *J. Bacteriol.* **171**, 1245–1253.
35. Schmidheini, T., Mosch, H.-U., Evans, J.N.S. & Braus, G. (1990). Yeast allosteric chorismate mutase is locked in the activated state by a single amino acid substitution. *Biochemistry* **29**, 3660–3668.
36. Richards, T.I., Layden, K., Werminski, E.E., Milburn, P.J. & Haslam, A. (1987). The shikimate pathway. Part 7. Chorismate mutase: towards an enzyme model. *J. Chem. Soc. Perkin Trans.* **I**, 2765–2773.
37. Hilvert, D., Carpenter, S.H., Nared, K.D. & Auditor, M.-T.M. (1988). Catalysis of concerted reactions by antibodies: the Claisen rearrangement. *Proc. Natl. Acad. Sci. USA* **85**, 4953–4955.
38. Jackson, D.Y., Jacobs, J.W., Sugasawara, R., Reich, S.H., Bartlett, P. A. & Schultz, P.G. (1988). An antibody-catalyzed Claisen rearrangement. *J. Am. Chem. Soc.* **110**, 4841–4842.
39. Bowdish, K., Tang, Y., Hicks, J.B. & Hilvert, D. (1991). Yeast expression of a catalytic antibody with chorismate mutase activity. *J. Biol. Chem.* **266**, 11901–11908.
40. Haynes, M.R., Stura, E.A., Hilvert, D. & Wilson, I.A. (1994). Routes to catalysis: structure of a catalytic antibody and comparison with its natural counterpart. *Science* **263**, 646–652.
41. Jackson, D.Y., Liang, M.N., Bartlett, P.A. & Schultz, P.G. (1992). Activation parameters and stereochemistry of an antibody-catalyzed

Claisen rearrangement. *Angew. Chem. Int. Ed. Engl.* **31**, 182–183.
42. Lee, A.Y., Karplus, A.P., Ganem, B. & Clardy, J. (1995). Atomic structure of the buried catalytic pocket of *Escherichia coli* chorismate mutase. *J. Am. Chem. Soc.* **117** 3627–3628.
43. Burrows, C.J. & Carpenter, B.K. (1981). Substituent effects on the aliphatic Claisen rearrangement. 1. Synthesis and rearrangement of cyano-substituted allyl vinyl ethers. *J. Am. Chem. Soc.* **103**, 6983–6984.
44. Gray, J.V., Golinelli-Pimpaneau, B. & Knowles, J.R. (1990). Monofunctional chorismate mutase from Bacillus subtilis: purification of the protein and molecular cloning of the gene, and overexpression of the gene product in *Escherichia coli*. *Biochemistry* **29**, 376–383.
45. Stewart, J.D., Wilson, D.B. & Ganem, B. (1990). A genetically engineered monofunctional chorismate mutase. *J. Am. Chem. Soc.* **112**, 4582–4584.
46. Breslow, R. & Hoffman, Jr, J.M. (1972). Solvolytic Cope rearrangements. *J. Am. Chem. Soc.* **94**, 2111–2112.
47. Goering, H.L. & Jacobson, R.R. (1958).A kinetic study of the *ortho*-Claisen rearrangement. *J. Am. Chem. Soc.* **80**, 3277–3285.
48. White, W.N., Gwynn, D., Schlitt, R., Girard, C. & Fife, W. (1958). The *ortho*-Claisen rearrangement. I. The effect of substituents on the rearrangement of allyl p-X-phenyl ethers. *J. Am. Chem. Soc.* **80**, 3271–3277.
49. Coates, R.M., Rogers, B.D., Hobbs, S.J., Peck, D.R. & Curran, D.P. (1987). Synthesis and Claisen rearrangement of alkoxyallyl enol ethers. Evidence for a dipolar transition state. *J. Am. Chem. Soc.* **109**, 1160–1170.
50. Brandes, E., Grieco, P.A. & Gajewski, J.J. (1989). Effect of polar solvents on the rates of Claisen rearrangements: assessment of ionic character. *J. Org. Chem.* **54**, 515–516.
51. Gajewski, J.J. & Brichford, N.L. (1994). Secondary deuterium kinetic isotope effects in the aqueous Claisen rearrangement: evidence against an ionic transition state. *J. Am. Chem. Soc.* **116**, 3165–3166.
52. Severance, D.L. & Jorgensen, W.L. (1992). Effects of hydration on the Claisen rearrangement of allyl vinyl ether from computer simulations. *J. Am. Chem. Soc.* **114**, 10966–10968.
53. Dodziuk, H., Von Voithenberg, H. & Allinger, N.L. (1982). A molecular mechanics study of methyl vinyl ether and related compounds. *Tetrahedron* **38**, 2811–2819.

Angela Y Lee, Jon D Stewart, Jon Clardy and Bruce Ganem, Department of Chemistry, Baker Laboratory, Cornell University, Ithaca, NY 14853-1301, USA.